

DESIGN AND IMPLEMENTATION OF AN ISOLATED WIND-HYDRO HYBRID SYSTEM

¹Sharan Kumar S. S, ²Suchitra S. S

^{1,2}Integrated M.Tech V/V - P.E.E, School of Engineering, Central University of Karnataka-585367, India.

Abstract: This paper presents the design and implementation of an isolated wind-hydro hybrid system using matlab/simulink. The proposed wind-hydro hybrid system consists of a battery energy storage system (BESS) in between two back-back power converter. One converter is placed at source side (called source converter) an other converter is place at load side (Called load converter). The aim of the source converter is to track the maximum power point(MPP) from the variable source of wind energy and the aim of the load converter is to achieve the voltage/frequency(v/f) control.

Keywords: renewable energy sources (RES), hybrid systems, battery energy storage system (BESS), Maximum power point tracking (MPPT), voltage/frequency(v/f) control.

I. Introduction

The global warming issue is well known to developing countries across the world. The energy production fossil fuels burning in one of vital issue causing pollution leading global warming. Generation of clean energy from renewable energy (RE) sources like wind, hydro, biomass, solar etc is the optimal solution for the cause. Electric utilities and end users of electric power are becoming increasingly concerned about meeting the growing energy demand [1]-[2]. Among the RE sources based power generation systems, wind and hydro have the ability to complements each other in stand-alone applications. Battery energy storage systems (BESS) are becoming popular in various aspects of the power system issues [3]-[5].

For power generation by small hydro or micro hydro as well as wind systems, the use of squirrel cage induction generators (SCIGs) has been reported in literature [6], [7]. In the case of stand-alone or autonomous systems, the issues of voltage and frequency control (VFC) are very important. A battery-based controller is proposed for control of voltage and frequency in the isolated wind energy conversion systems (WECS). However, maximum power point tracking (MPPT) could not be realized in this battery-based isolated system employing SCIG operated at fixed speed [7], [8].

Over view of this paper is organized as follows. Significance of RE based systems, hybrid systems with BESS is discussed in Section 1. System configuration and principles of operation is given in the Section 2. MATLAB/Simulink based output results of proposed wind-hydro hybrid system are given in Section 3. Conclusion is given in the Section 4.

II. Wind-Hydro hybrid system configuration and operation

In this paper, the subscript 'w' is used to denote the parameters and variables of wind turbine generator and subscript 'h' is used to denote the parameters and variables of hydro turbine generator.

The two back-to-back connected Pulse Width Modulations (PWM) controlled Insulated Gate Bipolar Transistor (IGBT) based Voltage Source Converters (VSCs) are connected between the stator windings of $SCIG_w$ at wind power generation side (machine side) and the stator windings of $SCIG_h$ at hydro power generation (load side) to facilitate bidirectional power flow. The stator windings of the $SCIG_h$ are connected to the load terminals at hydro power generation side. The two VSCs may be called as the machine side converter at $SCIG_w$ and the load side converter at $SCIG_h$.

2.1. Machine Side Converter Control Technique:

The objectives of the machine ($SCIG_w$) side converter are to achieve optimum torque for MPT for $SCIG_w$ and to provide the required magnetizing current to the $SCIG_w$.

A. Speed-Control Loop for MPPT :

In the proposed algorithm, the rotor position (θ_{rw}) of $SCIG_w$ and the wind speed are sensed. The rotor speed (ω_{rw}) of $SCIG_w$ is determined from its rotor position (θ_{rw}). The tip speed ratio (λ_w) for a wind turbine of radius (r_w) and gear ratio (η_w) at a wind speed of v_w is defined as [9]-[13].

$$\lambda_w = \frac{\omega_{rw} r_w}{\eta_w v_w} \quad (1)$$

For MPPT in the wind-turbine-generator system, the $SCIG_w$ should operate at the optimum tip speed ratio (λ_w^*) Thus the reference rotor speed (ω_{rw}^*) for MPT is generated using equation 1 as

$$\lambda_w^* = \frac{\omega_{rw}^* r_w}{\eta_w v_w} \quad (2)$$

The flow chart diagram for the proposed MPT technique is given in Fig.1

B. Reference q-axis $SCIG_w$ Stator-Current Generation:

The reference rotor speed of $SCIG_w$ is compared with (ω_{rw}) to calculate the rotor-speed error (ω_{rwer}) at the n^{th} sampling instant as

$$\omega_{rwer(n)} = \omega_{rw}^*(n) - \omega_{rw}(n) \quad (3)$$

The aforementioned error is fed to the speed proportional integral (PI) controller. At the n^{th} sampling instant, the output of the speed PI controller with proportional gain $K_{p\omega}$ and integral gain $K_{i\omega}$ gives the reference q-axis $SCIG_w$ stator current (I_{qsw}^*).

B. Reference d-axis SCIG_w Stator-Current Generation:

The reference d-axis SCIG_w stator current (I_{dsw}^*) is determined from the rotor flux set point (φ_{drw}^*) at the n^{th} sampling instant as

$$I_{dsw(n)}^* = \frac{\varphi_{drw}^*}{L_{mw}} \tag{4}$$

Where L_{mw} is the magnetizing inductance of SCIG_w

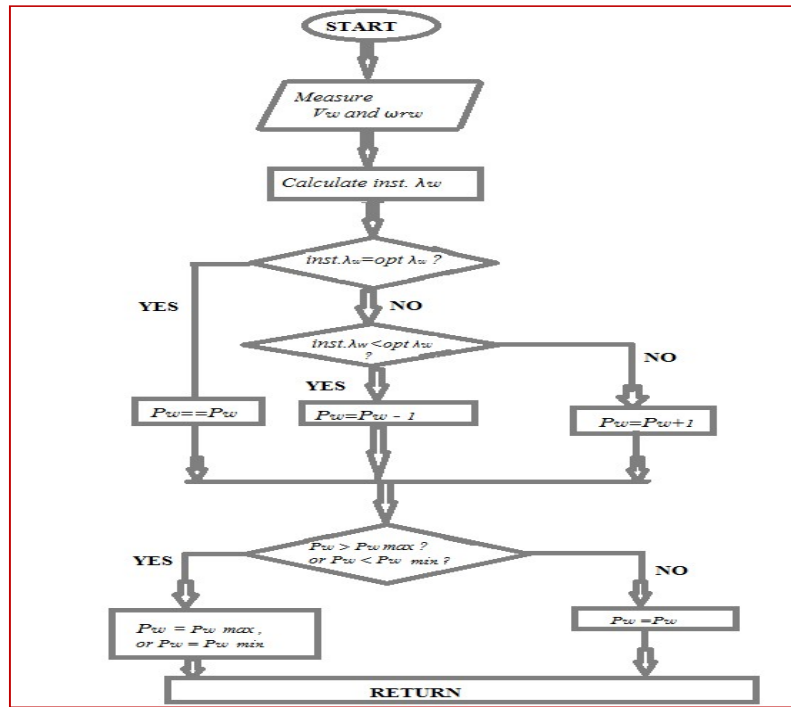


Fig.1. Flow chart diagram of MPPT technique.

C. Generation of PWM Signal for Machine-Side Converter:

For generation of three-phase reference SCIG_w stator currents (i_{swa}^* , i_{swb}^* , and i_{swc}^*), the transformation angle $\theta_{rotorflux w}$ is

$$\theta_{rotor flux w} = \theta_{slip w} + \left(\frac{pw}{2}\right) \theta_{rw} \tag{5}$$

The references for d-q components of SCIG_w stator currents are converted as

$$i_{swa}^* = I_{dsw}^* \sin(\theta_{rotor flux w}) + I_{qsw}^* \cos(\theta_{rotor flux w}) \tag{6}$$

$$i_{swb}^* = I_{dsw}^* \sin(\theta_{rotor flux w} - 2\pi/3) + I_{qsw}^* \cos(\theta_{rotor flux w} - 2\pi/3) \tag{7}$$

$$i_{swc}^* = I_{dsw}^* \sin(\theta_{rotor flux w} + 2\pi/3) + I_{qsw}^* \cos(\theta_{rotor flux w} + 2\pi/3) \tag{8}$$

The three-phase reference SCIG_w stator currents (i_{swa}^* , i_{swb}^* , and i_{swc}^*) are then compared with the sensed SCIG_w stator currents (i_{swa} , i_{swb} and i_{swc}) to compute the SCIG_w stator current errors, and these current errors are amplified with gain ($K = 5$) and the amplified signals are compared with a fixed frequency (10 kHz) triangular carrier wave of unity amplitude to generate gating signals for the IGBTs of the machine-side VSC. The sampling time of the controller is taken as 50 μs, as this time is sufficient for completion of calculations in a typical DSP controller. The total control mechanism of machine side converter is shown in Fig.2

2.2. Load-Side Converter Control Technique:

The objectives of the load-side converter are to maintain rated voltage and frequency at the load terminals irrespective of connected load. The power balance in the system is maintained by diverting the surplus power generated to the battery or by supplying power from the battery in case of deficit between generated power and load requirement. Similarly, the required reactive power for the load is supplied by the load-side converter to maintain constant value of the load voltage [9]-[13].

A. Generation of Reference Three-Phase SCIG_w Currents:

The reference voltages (v_{an}^* , v_{bn}^* and v_{cn}^*) for the control of the load voltages at time t are given as

$$v_{an}^* = \sqrt{2} v_t \sin(2\pi ft) \tag{9}$$

$$v_{bn}^* = \sqrt{2} v_t \sin(2\pi ft - 120^\circ) \tag{10}$$

$$v_{cn}^* = \sqrt{2} v_t \sin(2\pi ft + 120^\circ) \tag{11}$$

where f is the nominal frequency (50Hz) and v_t is the phase-neutral load voltage, which is 240 V.

The load voltages (v_{an} , v_{bn} and v_{cn}) are sensed and compared with the reference voltages. The error voltages (v_{anerr} , v_{bnerr} and v_{cnerr}) at the n^{th} sampling instant are calculated as

$$v_{anerr}(n) = \{v_{an}^*(n) - v_{an}(n)\} \tag{12}$$

$$v_{bnerr}(n) = \{v_{bn}^*(n) - v_{bn}(n)\} \tag{13}$$

$$v_{cnerr}(n) = \{v_{cn}^*(n) - v_{cn}(n)\} \tag{14}$$

The reference three-phase SCIG_n currents (i_{sha}^* , i_{shb}^* and i_{shc}^*) are generated by feeding the voltage error signals to PI voltage controller with proportionate gain K_{pv} and integral gain K_{iv} .

The reference three-phase SCIG_n currents are then compared with the sensed SCIG_w currents (i_{sha} , i_{shb} and i_{shc}) to compute the SCIG_w current errors as

$$i_{shae} = i_{sha}^* - i_{sha} \tag{15}$$

$$i_{shber} = i_{shb}^* - i_{shb} \tag{16}$$

$$i_{shcer} = i_{shc}^* - i_{shc} \tag{17}$$

These current errors are amplified with gain ($K=5$), and the amplified signals are compared with a fixed-frequency (10 kHz) triangular carrier wave of unity amplitude to generate gating signals for IGBTs of the load-side converter. The sampling time of the controller is taken as $50 \mu s$, as this time is sufficient for completion of calculations in a typical DSP controller. The total load side converter control mechanism is shown in Fig.3.

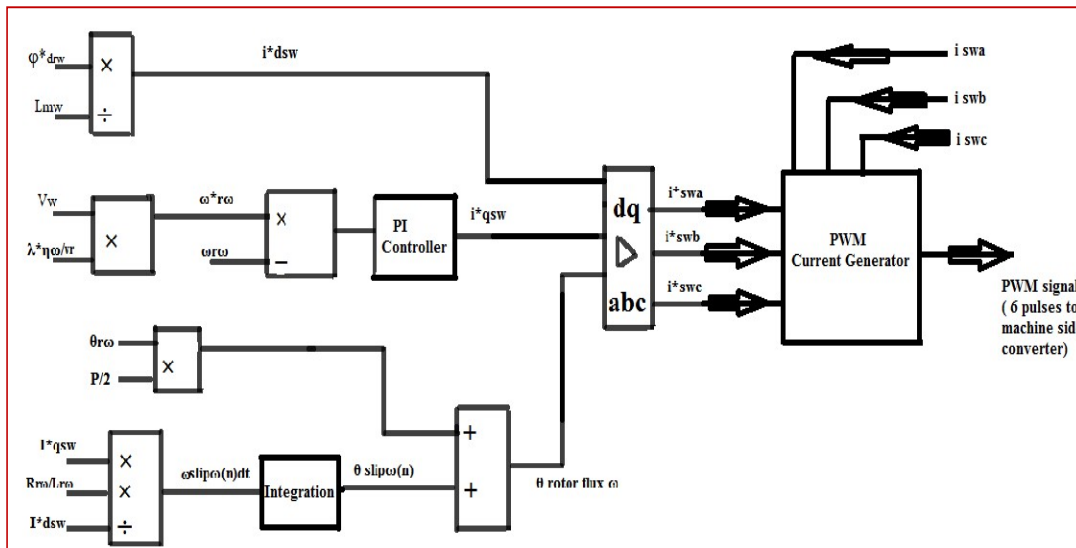


Fig. 2. Control Scheme of Machine side converter

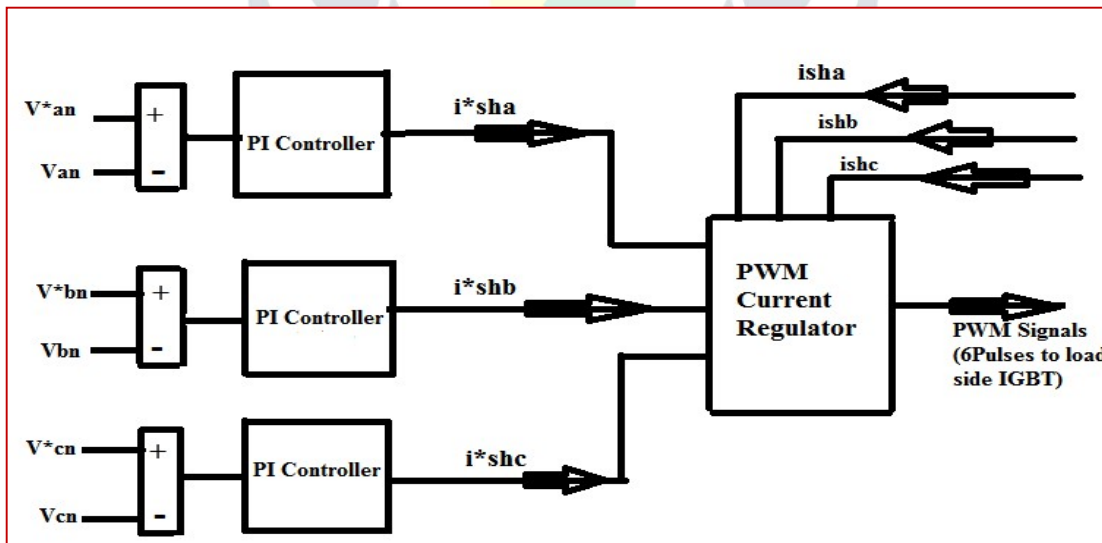


Fig. 3. Control Scheme of load side converter

3.3. Design Parameters:

1. Parameter of 37.3-kW 415-V 50-Hz Y-connected SCIGh: $R_s=0.09961\Omega$, $R_r=0.058 \Omega$, $L_s=0.869 \text{ mH}$, $L_r=0.030369 \text{ H}$, and Inertia=0.4 kg.m².
2. Parameters of 55-kW 415-V 50-Hz, Y-connected six-pole SCIG_w: $R_s = 0.059\Omega$, $L_s=0.687\text{mH}$, $R_r=0.0513\Omega$, $L_m=0.0298 \text{ H}$, and Inertia =1.5 kg.m².
3. Parameters of 55-kW wind turbine: wind speed range = 6.0-12m/s, speed range = 43-81r/min, $I=13.5 \text{ kg.m}^2$, $r = 7.5 \text{ m}$, $C_{pmax}=0.04412$, and $\lambda^*=5.66$.
4. BESS specifications: $C_b=43156 \text{ F}$, $R_b=10\text{k}\Omega$, $R_{in}=0.2\Omega$, $V_{oc \text{ max}} = 750\text{V}$, $V_{oc \text{ mix}} = 680\text{V}$, Storage = 600 kW.h, $L = 1 \text{ mH}$.

5. PI Controllers: $K_{pv} = 15$ and $K_{iv} = 0.05$.

6. Transformer Specifications: three single phase transformer of 15 kVA 138/138 V, connected in zig-zag manner.

III. Simulation Results of wind-hydro hybrid system

This sections converse the MATLAB/Simulink based results of the designed system. Simulation diagram of wind-hydro hybrid system is shown in Fig 5.

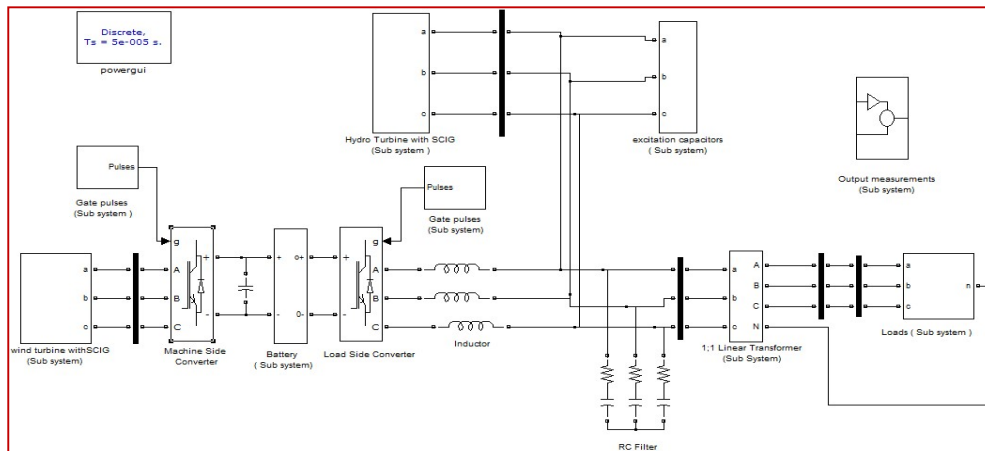
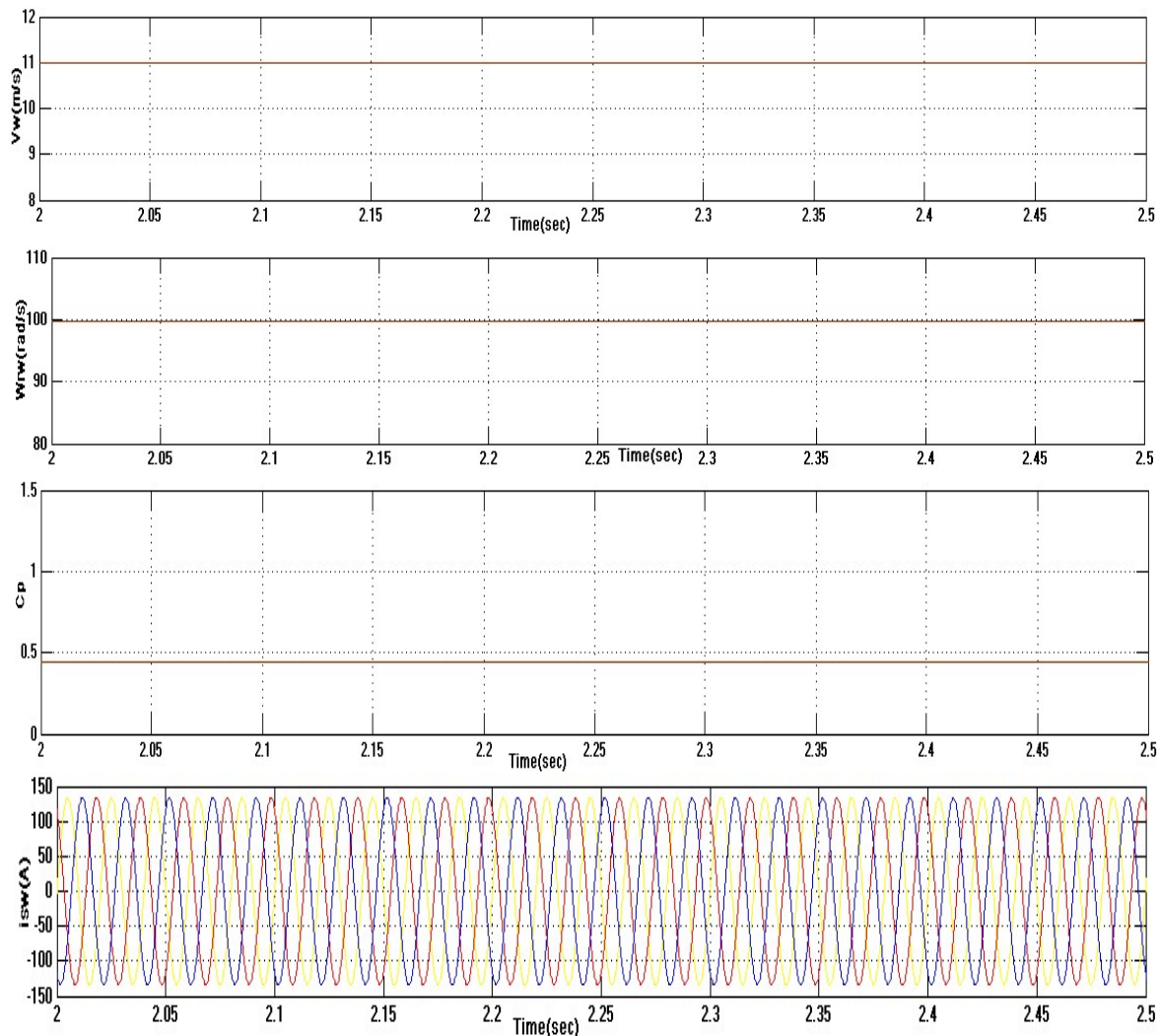
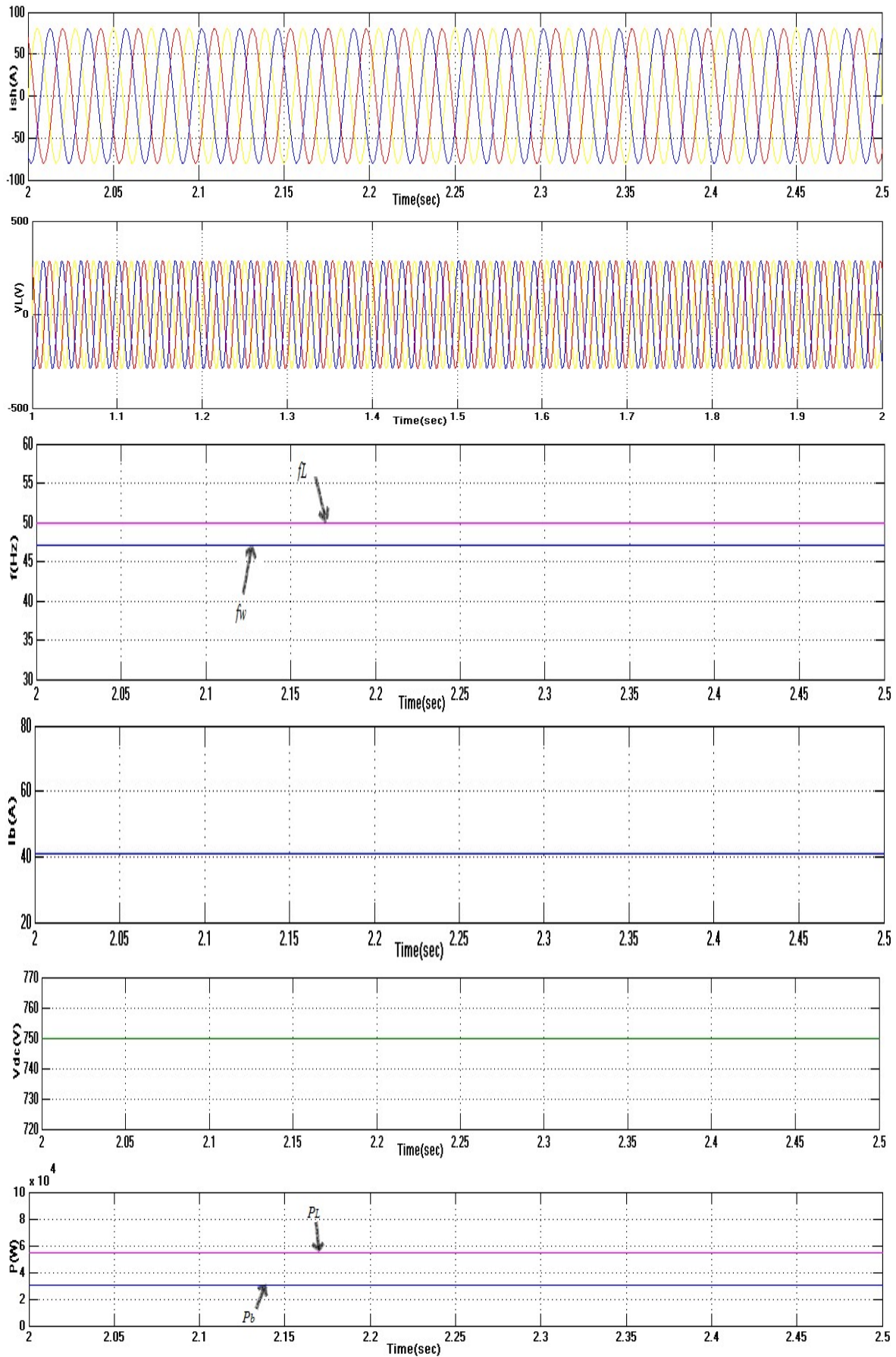


Fig 4. MATLAB/Simulink diagram of wind-hydro hybrid system with masked blocks

In Fig.5, the performance of the wind-hydro hybrid system with subscript value is shown with balanced linear load at wind speed of 11 m/s. The reactive power required by the load is supplied by the load-side converter to maintain the magnitude of the load voltage constant. Thus, under these conditions, both the magnitude and the frequency of the load voltage are maintained constant.





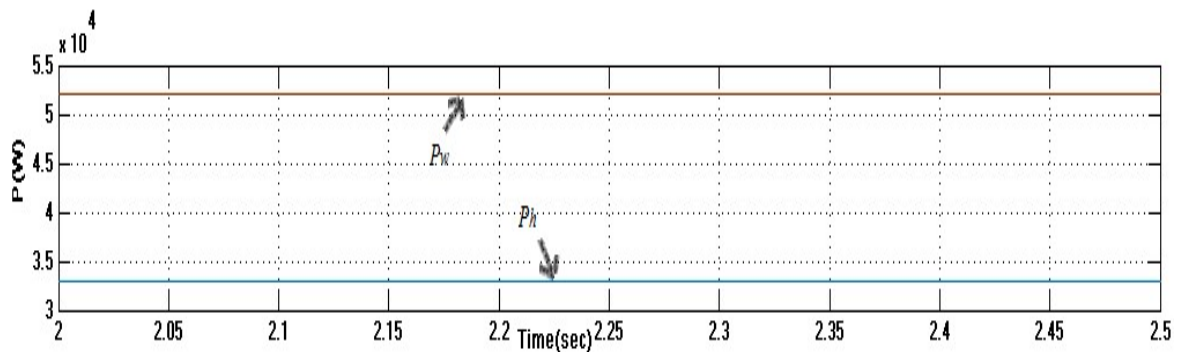


Fig.5. MATLAB Results of hybrid system with balanced linear load at wind speed of 11m/s

IV. Conclusion

In this paper, a three phase four wire local load wind-hydro hybrid system, using one squirrel cage induction generator driven by wind turbine and another squirrel cage induction generator driven by hydro turbine along with BESS and back-to-back power converter set, has been modeled and simulated in MATLAB software using Simulink and Sim Power System tool boxes.

References

- [1] Sandeep. V, Bala Murali Krishna. V, Kiran Kumar Namala and Nageswara Rao. D, "Grid Connected Wind Power System driven by PMSG with MPPT Technique using Neural Network Compensator", IEEE 2016, pp. 917-921.
- [2] Bala Murali Krishna .V, A. Sri Hari Babu , J. Jithendranath and Ch. Uma Maheswara Rao , " An Isolated Wind Hydro Hybrid System with Two Back-to-Back Power Converters and a Battery Energy Storage System Using Neural Network Compensator" , 2014 IEEE , pp.273-279.
- [3] Bala Murali Krishna. V et. at., "Cost Optimization by Integrating PV-System and Battery Energy Storage System into Microgrid using Particle Swarm Optimization", International Journal of Pure and Applied Mathematics Volume 114 No. 8 2017, pp. 45-55.
- [4] M. Black and G. Strbac, "Value of bulk energy storage for managing wind power fluctuations," IEEE Trans. Energy Convers., vol. 22, no. 1, pp. 197–205, Mar. 2007.
- [5] G. Quinonez-Varela and A. Cruden, "Modeling and validation of a squirrel cage induction generator wind turbine during connection to the local grid," IET Genre., Transmits. Distrib., vol. 2, no. 2, pp. 301–309, Mar. 2008.
- [6] J.B. Ekanayake, "Induction generators for small hydro schemes," IEEE Power Eng. J., vol. 16, no. 2, pp. 61–67, 2002.
- [7] D. Joshi, K. S. Sindhu, and M. K. Soni, "Constant voltage constant frequency operation for a self-excited induction generator," IEEE Trans. Energy Convers., vol. 21, no. 1, pp. 228–234, Mar. 2006.
- [8] L. A. C. Lopes and R. G. Almeida, "Wind-driven induction generator with voltage and frequency regulated by a reduced rating voltage source inverter," IEEE Trans. Energy Convers., vol. 21, no. 2, pp. 297–304, Jun. 2006.
- [9] Bhim Singh and V. Rajgopal, "Digital Control of Voltage and Frequency of Induction Generator in Isolated Small Hydro System," 2012 IEEE International Conference on Power Electronics, Drives and Energy System, vol.no1, pp 4673-4508.
- [10] Sreekala. C and Anju Mathew, "Voltage and frequency control of wind hydro hybrid system in isolated location using cage generators", 2013 IEEE pp 132-137.
- [11] Puneet K. Goel, Bhim Singh , S. S. Murthy and Navin Kishore, "Autonomous Hybrid System Using SCIG for Hydro Power Generation and Variable Speed PMSG for Wind Power Generation" IEEE 2009 PEDS pp 55-60.
- [12] B. Singh and G. K. Kasal, "Voltage and frequency controller for a three-phase four-wire autonomous wind energy conversion system," IEEE Trans. Energy Convers., vol. 23, no. 2, pp. 505–518, Jun. 2008.
- [13] Puneet K. Goel, Bhim Singh, S. S. Murthy and Navin Kishore , "Isolated Wind-Hydro Hybrid System Using Cage Generators and Battery Storage", IEEE Transactions on Industrial Electronics, vol. 58, No. 4, April 2011 , pp.1141-1153.